

Open system dynamics and quantum jumps: Divisibility vs. dissipativity

Dariusz Chruściński,^{1,*} Kimmo Luoma,^{2,†} Jyrki Piilo,^{3,‡} and Andrea Smirne^{4,5,§}

¹*Institute of Physics, Faculty of Physics, Astronomy and Informatics,
Nicolaus Copernicus University, Grudziadzka 5/7, 87-100 Toruń, Poland*

²*Institut für Theoretische Physik, Technische Universität Dresden, D-01062, Dresden, Germany*

³*Turku Center for Quantum Physics, Department of Physics and Astronomy,
University of Turku, FI-20014, Turun Yliopisto, Finland*

⁴*Dipartimento di Fisica “Aldo Pontremoli”, Università degli Studi di Milano, Via Celoria 16, I-20133 Milan, Italy*

⁵*Istituto Nazionale di Fisica Nucleare, Sezione di Milano, Via Celoria 16, I-20133 Milan, Italy*

Several key properties of quantum evolutions are characterized by divisibility of the corresponding dynamical maps. In particular, a Markovian evolution respects CP-divisibility, whereas breaking of P-divisibility provides a clear sign of non-Markovian effects. We analyze a class of evolutions which interpolates between CP- and P-divisible classes and is characterized by dissipativity – a long known but so far not widely used formal concept to classify open system dynamics. By making a connection to stochastic jump unravellings of master equations, we demonstrate that there exists inherent freedom in how to divide the terms of the underlying master equation into the deterministic and jump parts for the stochastic description. This leads to a number of different unravelings, each one with a measurement scheme interpretation and highlighting different properties of the considered open system dynamics. Starting from formal mathematical concepts, our results allow us to get fundamental insights in open system dynamics and to ease their numerical simulations.

Introduction.— Quantum jumps provide a powerful and insightful tool to describe the dynamics of open quantum systems [1, 2]. In the quantum-jump unraveling, the open-system state satisfying an assigned master equation is expressed as the average of – in principle, infinitely many – trajectories of pure states, that consist of deterministic evolutions interrupted by discontinuous, randomly distributed jumps [3]. Quantum jumps have been observed in several experimental platforms [4–9] and are computationally convenient to solve high-dimensional master equations. Hence, quantum jumps are routinely used to describe, e.g., quantum optical [10] or open many-body systems [11]. If the jumps are frequent and small enough, one can recover a different stochastic description of the open-system evolution, characterized by diffusive trajectories [12–16].

In the standard quantum-jump method, named Monte Carlo wave function (MCWF), the state transformations induced by the jumps and their occurrence probabilities are directly fixed by the operators and the coefficients of the master equation [3, 10]. This allows one to associate each trajectory with a continuous selective measurement performed on the open system [17], so that the master equation can be interpreted as due to the action of a non-selective observer, replacing the environment. However, the very definition of MCWF calls for a master equation with positive coefficients. Under some regularity conditions, this requirement is equivalent to the completely-positive(CP)-divisibility of the dynamics [18–20], meaning that the dynamics can be decomposed into intermediate completely positive maps. CP-divisibility has been introduced within the context of the definition of quantum Markovianity [21, 22] and its validity implies

the absence of memory effects [18, 23, 24], i.e., any information leaked from the open system into the environment will not affect the evolution of the open system back.

While generalizations of MCWF to treat master equations with negative coefficients have been introduced [25, 26], the possibility to extend the continuous-measurement interpretation beyond the realm of CP-divisible evolutions has been extensively debated in the literature [27–29]. Only very recently, a systematic approach to read the quantum-jump unraveling of non-CP-divisible evolutions in terms of continuous measurements has been put forward [30]. The approach relies on the definition of a proper rate operator [31–33] and has hence been named rate operator quantum jumps (ROQJ). It is associated with a continuous-measurement interpretation which applies to any positive(P)-divisible dynamics [24, 34–36], i.e., dynamics that can be decomposed into intermediate maps which are positive, but not necessarily completely positive. Furthermore, ROQJ has been extended to general not necessarily P-divisible evolutions [30], and it can be used to treat certain non-CP-divisible dynamics [37–39] where other non-Markovian jump methods cannot be used.

The previous analysis suggests that different ways to formulate a (jump) unraveling are related with different features of the resulting open-system dynamics, but is it possible to draw a precise connection between the two? In this paper, we make a significant step forward in clarifying this issue, by showing the rich structure revealed by different forms of unraveling for the same master equation. We introduce a family of ROQJ unravelings defined by different rate operators, whose positivity signals different divisibility properties of the dynamical maps. Besides

CP- and P-divisibility, we consider the so-called dissipativity of the generator fixing the dynamics – a property that corresponds to the validity of the Kadison-Schwarz inequality for the dynamical maps [40]. Our results also imply that certain non-CP-divisible dynamics can be related with several alternative continuous-measurement procedures, involving qualitatively different sets of states, even in the long-time regime. Finally, some of the ROQJ unravelings we introduce are particularly convenient for the actual numerical implementation of the trajectories, since their deterministic part is fixed by a linear, non-Hermitian operator, which allows us to recover a favorable trait of the MCWF.

From Monte Carlo Wave Function to Rate Operator Quantum Jumps.— We start by recalling the standard quantum-jump unraveling, the MCWF method [3, 10], and the recently introduced ROQJ [30], which sets the notation and will be the basis for our following analysis.

Consider the evolution of a finite-dimensional open quantum system given by the time-local master equation $d\rho(t)/(dt) = \mathcal{L}_t(\rho(t))$, where \mathcal{L}_t is the generator

$$\mathcal{L}_t(\rho) = -i[H(t), \rho] + \mathcal{J}_t(\rho) - \frac{1}{2}\{\Gamma(t), \rho\}, \quad (1)$$

with $\mathcal{J}_t(\rho) = \sum_{\alpha=1}^{N^2-1} c_\alpha(t) L_\alpha(t) \rho L_\alpha^\dagger(t)$, $\Gamma(t) = \sum_{\alpha=1}^{N^2-1} c_\alpha(t) L_\alpha^\dagger(t) L_\alpha(t)$, N the dimension of the open-system Hilbert space \mathcal{H}_S , $H(t) = H^\dagger(t)$ and $L_\alpha(t)$ linear operators on \mathcal{H}_S , and $c_\alpha(t)$ real functions; importantly, the representation of the generator \mathcal{L}_t via $H(t)$, \mathcal{J}_t and $\Gamma(t)$ as in Eq.(1) is highly non-unique [1], see also App.A. The structure of the generator follows from the trace- and Hermiticity-preservation properties of the dynamics [41] $\Lambda_t = T \exp\left(\int_0^t d\tau \mathcal{L}_\tau\right)$ (T is the time-ordering operator); moreover, the functions $c_\alpha(t)$ can take negative values, yet with the resulting evolution being positive and even completely positive [1, 42]. On the other hand, under some regularity conditions [18–20], the positivity of the coefficients, $c_\alpha(t) \geq 0$ for every α , is equivalent to the CP-divisibility of the dynamics, i.e, for any $t \geq s \geq 0$ one has the decomposition $\Lambda_t = V_{t,s} \Lambda_s$, where the so-called propagator $V_{t,s}$ is completely positive and trace preserving; CP-divisibility has been identified with quantum Markovianity in [21, 22].

In the case of CP-divisible dynamics, the master equation fixed by Eq.(1) can be obtained via a proper unraveling, the well-known MCWF, consisting of discontinuous pure-state trajectories in \mathcal{H}_S . The deterministic parts of the trajectories are fixed by the non-Hermitian operator $K(t) = H(t) - \frac{i}{2}\Gamma(t)$, according to

$$|\psi(t)\rangle \rightarrow |\psi(t+dt)\rangle = \frac{(1 - iK(t)dt)|\psi(t)\rangle}{\|(1 - iK(t)dt)|\psi(t)\rangle\|}, \quad (2)$$

while the discontinuous parts, the jumps, are given by

$$|\psi(t)\rangle \rightarrow |\psi(t+dt)\rangle = \frac{L_\alpha(t)|\psi(t)\rangle}{\|L_\alpha(t)|\psi(t)\rangle\|}, \quad (3)$$

and each jump occurs between t and $t + dt$ with probability

$$p_{\psi(t),\alpha} = c_\alpha(t) \|L_\alpha(t)|\psi(t)\rangle\|^2 dt; \quad (4)$$

here dt is meant to be an infinitesimal time increment and the probabilities are conditioned on the pre-jump state $|\psi(t)\rangle$ at time t .

It is clear that the previous formulation, in particular Eq.(4), requires all the rates to be positive. Recently [30], a different quantum-jump unraveling, named ROQJ, has been defined, weakening considerably such a requirement. ROQJ relies on the definition of the rate operator

$$\mathbf{W}_\psi = \sum_{\alpha=1}^{N^2-1} c_\alpha(t) (L_\alpha(t) - \ell_{\psi,\alpha}) P_\psi (L_\alpha(t) - \ell_{\psi,\alpha}(t))^\dagger, \quad (5)$$

with $\ell_{\psi,\alpha}(t) = \langle \psi | L_\alpha(t) | \psi \rangle$ and the projector $P_\psi = |\psi\rangle\langle\psi|$. As a first remark, which will be important in the following, we observe that \mathbf{W}_ψ is directly associated with the time-local generator \mathcal{L}_t and does not depend on its specific representation via $H(t)$, \mathcal{J}_t and $\Gamma(t)$: in fact, it can be equivalently written as

$$\mathbf{W}_\psi = (\mathbb{1} - P_\psi) \mathcal{L}_t(P_\psi) (\mathbb{1} - P_\psi), \quad (6)$$

i.e., using the projector P_ψ and the projector in the orthogonal complement, $(\mathbb{1} - P_\psi)$.

The building block of ROQJ is the observation that $\mathbf{W}_\psi \geq 0$ for any state vector $|\psi\rangle$ if and only if the corresponding dynamics is P-divisible [43], i.e., it can be decomposed as $\Lambda_t = V_{t,s} \Lambda_s$, and the propagator $V_{t,s}$ is trace preserving and positive, but not necessarily completely positive; P-divisibility, which is a significantly weaker requirement than CP-divisibility, has been identified with quantum Markovianity in [24, 36]. Focusing for now on P-divisible evolutions, one has then the spectral resolution $\mathbf{W}_{\psi(t)} = \sum_{k=1}^N \lambda_{\psi(t),k} |\varphi_{\psi(t),k}\rangle\langle\varphi_{\psi(t),k}|$ with $\lambda_{\psi(t),k} \geq 0$ for all $t \geq 0$. Introducing the non-Hermitian state-dependent operator $K_{\psi(t)} = K(t) + \Delta_{\psi(t)}$, with the non-linear correction $\Delta_{\psi(t)} = \frac{i}{2} \sum_{\alpha=1}^{N^2-1} c_\alpha(t) (2L_\alpha(t) \ell_{\psi,\alpha}^* - |\ell_{\psi,\alpha}^*|^2)$, one realizes the jump unraveling as follows [30]: the free evolution

$$|\psi(t)\rangle \rightarrow |\psi(t+dt)\rangle = \frac{(1 - iK_{\psi(t)}dt)|\psi(t)\rangle}{\|(1 - iK_{\psi(t)}dt)|\psi(t)\rangle\|} \quad (7)$$

is interrupted by the sudden jumps

$$|\psi(t)\rangle \rightarrow |\psi(t+dt)\rangle = \frac{V_{\psi(t),j}|\psi(t)\rangle}{\|V_{\psi(t),j}|\psi(t)\rangle\|}, \quad (8)$$

where $V_{\psi(t),j} = \sqrt{\lambda_{\psi(t),j}} |\varphi_{\psi(t),j}\rangle\langle\psi(t)|$; the probability that the jump j occurs between t and $t + dt$ is now $p'_{\psi(t),j} = \|V_{\psi(t),j}|\psi(t)\rangle\|^2 dt = \lambda_{\psi(t),j} dt$.

Compared to MCWF, the operators $L_\alpha(t)$ and rates $c_\alpha(t)$ are replaced in ROQJ by the eigenvectors and eigenvalues of the rate operator $\mathbf{W}_{\psi(t)}$, which allows one to formulate a well-defined unraveling for a wider set of dynamics. Moreover, in ROQJ the maximum number of types

of jumps, N , is smaller than in MCFW, $N^2 - 1$, which can represent a significant advantage for the numerical definition of the trajectories. Note that for both the MCWF [17] and the ROQJ [30] unraveling, the trajectories can be interpreted as due to a continuous measurement on the open system, i.e., the state transformations and corresponding probabilities can be associated with an instrument [44], mapping the set of outcomes into the set of open-system completely positive trace non-increasing maps. Finally, both methods can be extended to deal with, respectively, non-CP-divisible and non-P-divisible evolutions, via the use of reversed jumps connecting different trajectories [25, 26, 30]; however, such extensions lack a continuous-measurement interpretation.

A family of Rate Operator Quantum Jumps.— We now introduce a whole family of rate operators and corresponding unravelings, which bridge the gap between MCWF and ROQJ, and are related with different structural properties of the dynamics, as shown in the next paragraph.

The basic observation to define such rate operators is that \mathbf{W}_ψ in Eq.(6) can also be written as

$$\mathbf{W}_\psi = (\mathbb{1} - P_\psi)\mathbf{R}_\psi(\mathbb{1} - P_\psi), \quad (9)$$

where

$$\mathbf{R}_{\psi(t)} = \mathcal{J}_t(|\psi(t)\rangle\langle\psi(t)|). \quad (10)$$

Now, if $\mathbf{R}_{\psi(t)} \geq 0$ for any $|\psi(t)\rangle$ one can define another jump unraveling which merges (2)-(3) with (7)-(8); that is, the free evolution is governed by (2), but the jumps are realized via

$$|\psi(t)\rangle \rightarrow |\psi(t+dt)\rangle = \frac{R_{\psi(t),k}|\psi(t)\rangle}{\|R_{\psi(t),k}|\psi(t)\rangle\|}, \quad (11)$$

with $R_{\psi(t),k} = \sqrt{r_{\psi(t),k}}|\phi_{\psi(t),k}\rangle\langle\psi(t)|$, and the probability that the jump k occurs between t and $t+dt$ reads

$$p''_{\psi(t),k} = \|R_{\psi(t),k}|\psi(t)\rangle\|^2 dt = r_{\psi(t),k} dt; \quad (12)$$

indeed, $r_{\psi(t),k}$ and $|\phi_{\psi(t),k}\rangle$ are the eigenvalues and eigenvectors of $\mathbf{R}_{\psi(t)}$. The proof that the master equation (1) is recovered via the average over the trajectories is in App.B.

The unravelling now defined avoids the non-linear correction in the non-Hermitian operator fixing the deterministic evolution, still potentially allowing for positive probabilities in the case of non-CP-divisible evolutions; $p''_{\psi(t),k} \geq 0$ is in fact equivalent to the requirement that for all $t \geq 0$ the map \mathcal{J}_t is positive. Importantly, we note that the definition of the rate operator $\mathbf{R}_{\psi(t)}$ in Eq.(10) does depend on the specific choice of the map \mathcal{J}_t in the representation of the generator \mathcal{L}_t as in Eq.(1); as a consequence Eqs.(2), (11) and (12) define a family of unravelings characterized by different trajectories (see the examples below). To keep the nomenclature simple, we

will call each of these unravelings **R**-ROQJ, specifying the explicit form of the rate operator \mathbf{R} when needed; furthermore, we will refer to the ROQJ unraveling discussed in the previous paragraph as **W**-ROQJ.

Dissipativity vs. divisibility. — We now move on to the main purpose of our paper, i.e., deriving a clear connection between relevant properties of an open-system dynamics and the different forms of unraveling of the related master equation.

Clearly, if the evolution is CP-divisible, not only both MCWF and **W**-ROQJ are well defined, but one can always find a completely positive map \mathcal{J}_t giving rise to a positive **R**-ROQJ. Instead, any P-divisible evolution does guarantee positivity of $\mathbf{W}_{\psi(t)}$, but not necessarily the positivity of $\mathbf{R}_{\psi(t)}$. Still, P-divisibility constrains the number of possible negative eigenvalues of the rate operator $\mathbf{R}_{\psi(t)}$. We have in fact the following:

Proposition 1. *For any P-divisible evolution, $\mathbf{R}_{\psi(t)}$ can have at most one negative eigenvalue.*

For the proof see App.C. We want to stress here that the proof does not depend on the specific \mathcal{J}_t used to represent the generator \mathcal{L}_t and hence applies to any **R**-ROQJ.

A natural question is then whether there is a class of quantum evolutions guaranteeing the positivity of $\mathbf{R}_{\psi(t)}$. The answer to the question is affirmative and is provided by a class of evolutions which was already considered by Lindblad in his seminal paper [40]. As said, P-divisibility implies the existence of positive trace-preserving propagators $V_{t,s}$. Now, moving to the Heisenberg picture, the corresponding propagators $V_{t,s}^\dagger$ are positive and unital. There exists a special class of positive unital maps which satisfy the Kadison-Schwarz inequality

$$\Phi(X^\dagger X) \geq \Phi(X^\dagger)\Phi(X). \quad (13)$$

Actually, any unital hermiticity-preserving maps satisfying (13) is positive. However, the converse is not true (the transposition map is positive and unital, but does not satisfy (13)). The condition (13) is a natural generalization of $\langle X^\dagger X \rangle \geq \langle X^\dagger \rangle \langle X \rangle$, where $\langle X \rangle$ stands for the mean of the (in general non-Hermitian) operator X . The validity of the Kadison-Schwarz inequality for $V_{t,s}^\dagger$ directly translates into a definite property of the corresponding generator, according to the following.

Proposition 2. *The propagator $V_{t,s}^\dagger$ satisfies (13) for any $t \geq s$ if and only if the corresponding time-local generator \mathcal{L}_t^\dagger satisfies*

$$\mathcal{L}_t^\dagger(X^\dagger X) \geq \mathcal{L}_t^\dagger(X^\dagger)X + X^\dagger\mathcal{L}_t^\dagger(X), \quad (14)$$

for all $X \in \mathcal{B}(\mathcal{H})$ and $t \geq 0$.

The proof is a simple modification of arguments used in [40] for time-independent generators (see also [45]).

Now, following Lindblad [40] we call the time-local generator \mathcal{L}_t dissipative if the Heisenberg picture \mathcal{L}_t^\dagger satisfies (14) and k -dissipative if $\mathbb{1}_k \otimes \mathcal{L}_t$ is dissipative. Finally, \mathcal{L}_t is completely dissipative if it is k -dissipative for all k . If the system Hilbert space is N -dimensional, complete dissipativity is equivalent to N -dissipativity. This characterization is in parallel to k -divisibility [35]: the dynamical map Λ_t is k -divisible if the corresponding propagators $V_{t,s}$ are k -positive, that is, $\mathbb{1}_k \otimes V_{t,s}$ are positive. Then CP-divisibility is equivalent to N -divisibility. Now, k -dissipativity always implies k -divisibility for $k = 1, \dots, N-1$, and they coincide for $k = N$. The key result of our analysis is then the following.

Theorem 1. *If \mathcal{L}_t is dissipative, then there exists a representation (1) with a positive map \mathcal{J}_t , which we denote as \mathbf{J}_t .*

Proof. Let us recall the averaging procedure over the unitary group $U(N)$: $X \rightarrow \int_{U(N)} UXU^\dagger dU = \frac{1}{N} I \text{Tr} X$. Now (again following [40]), let us define $\mathbf{K}(t) = \int_{U(N)} \mathcal{L}_t^\dagger(U)U^\dagger dU$, and finally

$$\mathbf{J}_t^\dagger(X) = \mathcal{L}_t^\dagger(X) - (\mathbf{K}(t)X + X\mathbf{K}^\dagger(t)). \quad (15)$$

In App.D we show that \mathbf{J}_t defines a positive map. \square

In other terms, dissipativity guarantees the existence of a rate operator $\mathbf{R}_{\psi(t)}$, defined from \mathbf{J}_t by Eq.(10), such that the unraveling given by Eqs.(2), (11) and (12) is well-defined, as $\mathbf{R}_{\psi(t)} \geq 0$ for any $\psi(t)$.

Examples.— First, we consider the qubit evolution fixed by the generator [37–39]

$$\mathcal{L}_t(\rho) = \frac{1}{2} \sum_{k=1}^3 \gamma_k(t) (\sigma_k \rho \sigma_k - \rho), \quad (16)$$

where σ_k are the Pauli spin operators. We study the case where we have a P-divisible evolution even if one of the rates is temporally negative, i.e., CP-divisibility is broken; we suppose in particular that $\gamma_3(t) < 0$ for any $t > 0$. Then Λ_t is P-divisible provided that $\gamma_1(t), \gamma_2(t) \geq |\gamma_3(t)|$. Dissipativity requires the stronger condition [45] that $\gamma_1(t), \gamma_2(t) \geq 2|\gamma_3(t)|$. Interestingly, it turns out that whenever $\gamma_3(t) < 0$ the map $\mathcal{J}_t(\rho) = \sum_{k=1}^d \gamma_k(t) \sigma_k \rho \sigma_k$ is not positive. However, if the generator (16) gives rise to a P-divisible evolution, then applying (15) one easily finds the following positive map (cf. App.E)

$$\mathbf{J}_t(\rho) = \sum_{k=1}^3 \gamma_k(t) (J_k(\rho) + \rho) = \mathcal{J}_t(\rho) + \gamma(t)\rho, \quad (17)$$

where $J_k(\rho) = \frac{1}{2}(\sigma_k \rho \sigma_k + \rho)$, and $\gamma(t) = \sum_k \gamma_k(t)$. In particular for the so called eternally non-Markovian evolution [37, 39] defined by $\gamma_1 = \gamma_2 = 1$, and $\gamma_3(t) =$

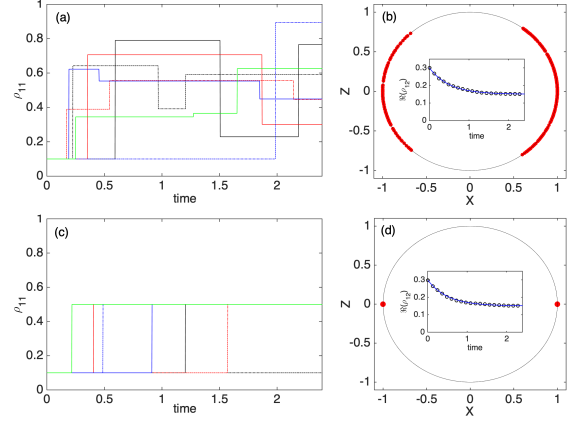


Figure 1. (Color online) Simulation results using rate operator $\mathbf{R1}$ [(a), (b)] and $\mathbf{R2}$ [(c), (d)]. Seven example pure state trajectories are displayed in (a) and (c) by plotting the probability of state $|1\rangle$. Final steady state distributions for Bloch vector X and Z components, with 500 trajectories, are shown in (b) and (d). Here, each dot corresponds to a single trajectory. In (d), all the 500 dots have the value $Z = 0$ and $X = -1/2$ or $X = +1/2$, i.e., we have only two distinctively visible dots. The insets in (b) and (d) demonstrate the agreement between the analytical and simulation results by using the coherence ρ_{12} and having 10^4 trajectories. In the insets, the solid line is the analytical result and the dots are the simulation results. The error bars are similar to the size of the dots. In all the panels, the initial state is $|\psi(0)\rangle = \sqrt{0.1}|1\rangle + \sqrt{0.9}|2\rangle$ and the used time step size is $dt = 0.002$.

$-\tanh t$, one has a P-divisible evolution, but the corresponding generator $\mathcal{L}_t^\dagger = \mathcal{L}_t$ is not dissipative. Nevertheless, the map \mathbf{J}_t is positive and one can define the positive rate operator

$$\mathbf{R1}_{\psi(t)} = \mathbf{J}_t(|\psi(t)\rangle\langle\psi(t)|) \geq 0. \quad (18)$$

The deterministic evolution includes $K1(t) = \frac{i}{2}[\gamma_1(t) + \gamma_2(t) + \gamma_3(t)]\mathbb{1}$ where $\mathbb{1}$ is the identity operator. Figure 1 (a) shows 7 example pure-state trajectories, with initial state $|\psi(0)\rangle = \sqrt{0.1}|1\rangle + \sqrt{0.9}|2\rangle$, and plotting the probability ρ_{11} of the state $|1\rangle$. During the time evolution, the probability covers the range of values $0.1 \leq \rho_{11} \leq 0.9$. Note that the quantum jumps continue between a specific set of states even when the system has essentially already reached the steady state. Figure 1 (b) displays the distribution of the final states of 500 trajectories in terms of the Bloch vector X and Z components. The inset of Fig. 1 (b) shows in detail the agreement between the analytical results of coherence ρ_{12} and simulations.

We can also define another positive rate operator

$$\mathbf{R2}_{\psi(t)} = \mathbf{R1}_{\psi(t)} - 2\gamma_3(t)|\psi(t)\rangle\langle\psi(t)|, \quad (19)$$

where the deterministic evolution includes now $K2(t) = \frac{i}{2}[\gamma_1(t) + \gamma_2(t)]\mathbb{1}$. The simulation results are shown in Fig. 1 (c) and (d). The example trajectories in Fig. 1

(c) illustrate that the ensemble consists now a discrete set of pure states and that the quantum jumps terminate when the steady state is reached. In the final distribution of states, see Fig. 1 (d), we have only two states $|\pm\rangle = \frac{1}{\sqrt{2}}(|1\rangle \pm |2\rangle)$. As a matter of fact, during the whole simulation, only three states appear: the initial state and $|\pm\rangle$. The inset of 1 (d) shows again the excellent agreement between the analytical result and simulations.

All this leads to the following fundamental conclusion. Not only there exist many different measurement schemes – along a number of positive rate operators – for the same master equation containing negative rates. Remarkably, the results with $\mathbf{R2}_{\psi(t)}$ explicitly demonstrate that the measurement basis can be fixed once and for all, without any state and time dependence; in the case with $\mathbf{R2}_{\psi(t)}$, it is the $|\pm\rangle$ basis. In App.G, we introduce another rate operator $\mathbf{R3}_{\psi(t)}$ and discuss in more detail the comparison between the different rate operators, including \mathbf{W}_{ψ} .

As second example, we consider the well-studied qubit evolution governed by

$$\begin{aligned} \mathcal{L}_t(\rho) = & -i\frac{\omega(t)}{2}[\sigma_z, \rho] + \gamma_+(t)\mathcal{L}_+(\rho) \\ & + \gamma_-(t)\mathcal{L}_-(\rho) + \gamma_z(t)\mathcal{L}_z(\rho), \end{aligned} \quad (20)$$

where $\mathcal{L}_{\pm}(\rho) = \sigma_{\pm}\rho\sigma_{\mp} - \frac{1}{2}\{\sigma_{\mp}\sigma_{\pm}\rho\}$ and $\mathcal{L}_z(\rho) = \sigma_z\rho\sigma_z - \rho$. This model describes a very general and physically-relevant qubit evolution, taking into account, besides the unitary evolution, the pumping \mathcal{L}_+ , damping \mathcal{L}_- , and dephasing \mathcal{L}_z contributions (see the recent analysis in [46–49]). Now, P-divisibility requires $\gamma_{\pm}(t) \geq 0$ for all t ; hence, only $\gamma_z(t)$ can be negative. Interestingly, P-divisibility provides the following constraint for $\gamma_z(t)$ [49]: $\sqrt{\gamma_+(t)\gamma_-(t)} + 2\gamma_z(t) \geq 0$ for all $t \geq 0$. Note that the formula (20) gives rise to the following map

$$\mathcal{J}_t(\rho) = \gamma_+(t)\sigma_+\rho\sigma_- + \gamma_-(t)\sigma_-\rho\sigma_+ + \gamma_z(t)\sigma_z\rho\sigma_z, \quad (21)$$

which is never positive when $\gamma_z(t) < 0$. However, when $\gamma_{\pm}(t) \geq 0$ and $\sqrt{\gamma_+(t)\gamma_-(t)} + 2\gamma_z(t) \geq 0$ the map

$$\mathbf{J}_t(\rho) = \mathcal{J}_t(\rho) + \frac{1}{2}[\gamma_+(t) + \gamma_-(t) + 2\gamma_z(t)]\rho \quad (22)$$

is positive (cf. App.F) and hence gives rise to a positive rate operator $\mathbf{R}_{\psi(t)}$.

Conclusions. — In this paper, we introduced a quantum-jump unraveling (denoted as \mathbf{R} -ROQJ) that interpolates between MCWF for CP-divisible dynamics and the rate-operator unraveling for P-divisible evolutions [30, 43]. \mathbf{R} -ROQJ guarantees a well-defined continuous-measurement interpretation for the class of quantum evolutions defined by the condition (14), that is strictly stronger than P-divisibility. Furthermore, \mathbf{R} -ROQJ considerably simplifies the deterministic part of the evolution between the jumps, that is fixed by a linear operator, as in MCWF. Interestingly, different rate

operators \mathbf{R}_{ψ} can reveal different features of the corresponding quantum evolution, in particular corresponding to different measurement schemes. In addition to fundamental insight to open system dynamics, our results also allow us to simplify numerical simulations for practical purposes.

D.C. was supported by the Polish National Science Centre project 2018/30/A/ST2/00837. J.P. acknowledges support from Magnus Ehrnrooth Foundation. A.S. acknowledges funding by the FFABR project of MIUR.

* darch@fizyka.umk.pl

† kimmo.luoma@tu-dresden.de

‡ jyrki.piilo@utu.fi

§ andrea.smirne@unimi.it

- [1] H.-P. Breuer and F. Petruccione, *The Theory of Open Quantum Systems* (Oxford Univ. Press, Oxford, 2007).
- [2] H.J. Carmichael, *An Open System Approach to Quantum Optics, Lectures Notes in Physics* (Springer, Berlin, 1993)
- [3] J. Dalibard, Y. Castin, and K. Mølmer, Phys. Rev. Lett. **68**, 580 (1992).
- [4] T. Basche, S. Kummer, and C. Brauchle, Nature **373**, 132 (1995).
- [5] S. Peil and G. Gabrielse, Phys. Rev. Lett. **83**, 1287 (1999).
- [6] F. Jelezko, I. Popa, A. Gruber, C. Tietz, J. Wrachtrup, A. Nizovtsev, and S. Kilin, Appl. Phys. Lett. **81**, 2160 (2002).
- [7] S. Gleyzes, S. Kuhr, C. Guerlin, J. Bernu, S. Deléglise, U.B. Hoff, M. Brune, J.-M. Raimond, and S. Haroche, Nature **446**, 297 (2007).
- [8] R. Vijay, D. H. Slichter, and I. Siddiqi, Phys. Rev. Lett. **106**, 110502 (2011).
- [9] Z. K. Mineev, S. O. Mundhada, S. Shankar, P. Reinhold, R. Gutiérrez-Jáuregui, R.J. Schoelkopf, M. Mirrahimi, H. J. Carmichael, and M. H. Devoret, Nature **570**, 200 (2019).
- [10] M. B. Plenio and P. L. Knight, Rev. Mod. Phys. **70**, 101 (1998).
- [11] A.J. Daley, Adv. Phys. **63**, 77 (2014).
- [12] I.Percival, *Quantum State Diffusion* (Cambridge University Press, Cambridge, England, 2002)
- [13] A. Barchielli and M. Gregoratti, *Quantum Trajectories and Measurements in Continuous Time: The Diffusive Case*, Lecture Notes in Physics 782 (Springer, Berlin, 2009).
- [14] W. T. Strunz, L. Diósi, and N. Gisin, Phys. Rev. Lett. **82**, 1801 (1999).
- [15] T. Yu, L. Diósi, N. Gisin, and W. T. Strunz, Phys. Rev. A **60**, 91 (1999).
- [16] K. Luoma, W.T. Strunz, J. Piilo, arXiv:2004.12072, in press in Phys. Rev. Lett.
- [17] A. Barchielli and V.P. Belavkin, J. Phys. A: Math. Gen. **24** 1495 (1991).
- [18] E.-M. Laine, J. Piilo, and H.-P. Breuer, Phys. Rev. A **81**

- 062115 (2010).
- [19] D. Chrusciński, A. Kossakowski, and Á. Rivas, Phys. Rev. A **83**, 052128 (2011)
- [20] Á. Rivas and S. F. Huelga, *Open Quantum Systems* (Springer, New York, 2012).
- [21] Á. Rivas, S. F. Huelga, and M. B. Plenio, Phys. Rev. Lett. **105**, 050403 (2010).
- [22] Á. Rivas, S. F. Huelga, and M. B. Plenio, Rep. Prog. Phys. **77**, 094001 (2014)
- [23] H.-P. Breuer, E.-M. Laine, and J. Piilo, Phys. Rev. Lett. **103**, 210401 (2009);
- [24] H.-P. Breuer, E.-M. Laine, J. Piilo, and B. Vacchini, Rev. Mod. Phys. **88**, 021002 (2016).
- [25] J. Piilo, S. Maniscalco, K. Härkönen, K.-A. Suominen, Phys. Rev. Lett. **100**, 180402 (2008).
- [26] J. Piilo, K. Härkönen, S. Maniscalco, K.-A. Suominen, Phys. Rev. A **79**, 062112 (2009).
- [27] J. Gambetta and H.M. Wiseman, Phys. Rev. A **68**, 062104 (2003).
- [28] L. Diósi, Phys.Rev.Lett. **100**, 080401 (2008).
- [29] H.M. Wiseman and J.M. Gambetta, Phys. Rev. Lett. **101**, 140401 (2008).
- [30] A. Smirne, M. Caiaffa, and J. Piilo, Phys. Rev. Lett. **124**, 190402 (2020).
- [31] L. Diósi, Phys. Lett. A **114**, 451 (1986).
- [32] L. Diósi, J. Phys. A **21**, 2885 (1988).
- [33] N. Gisin, Helv. Phys. Acta **63** 929 (1990).
- [34] B. Vacchini, A. Smirne, E.-M. Laine, J. Piilo, H.-P. Breuer, New J. Phys. **13**, 093004 (2011).
- [35] D. Chrusciński and S. Maniscalco, Phys. Rev. Lett. **112**, 120404 (2014).
- [36] S. Wißmann, H.-P. Breuer, B. Vacchini, Phys. Rev. A **92**, 042108 (2015).
- [37] M.J.W. Hall, J.D. Cresser, L. Li, and E. Andersson, Phys. Rev. A **89**, 042120 (2014).
- [38] D. Chrusciński and F.A. Wudarski, Phys.Rev. A **91**, 012104 (2015).
- [39] N. Megier, D. Chruscinski, J. Piilo, and W.T. Strunz, Sci. Rep. **7**, 6379 (2017).
- [40] G. Lindblad, Comm. Math. Phys. **48**, 119 (1976).
- [41] V. Gorini, A. Kossakowski, and E. C. G. Sudarshan, J. Math. Phys. **17**, 821 (1976).
- [42] D. Chrusciński, and A. Kossakowski, Phys. Rev. Lett. **104**, 070406 (2010).
- [43] M. Caiaffa, A. Smirne, A. Bassi, Phys. Rev. A **95** 062101 (2017).
- [44] T. Heinosaari and M. Ziman, *The Mathematical Language of Quantum Theory*, (Cambridge University Press, Cambridge, 2012).
- [45] D. Chrusciński, F. Mukhamedov, Phys. Rev. A. **100**, 052120 (2019).
- [46] A. Smirne, J. Kolodyński, S.F. Huelga, and R. Demkowicz-Dobrzanski, Phys. Rev. Lett. **116**, 120801 (2016).
- [47] J.F. Haase, A. Smirne, J. Kolodyński, R. Demkowicz-Dobrzanski, and S.F. Huelga, New J. Phys. **20**, 053009 (2018).
- [48] J. Teittinen, H. Lyyra, B. Sokolov, and S. Maniscalco, New J. Phys. **20**, 073012 (2018).
- [49] S. N. Filippov, A.N. Glinov, and L. Leppäjärvi, Lobachevskii Journal of Mathematics, **41**, 617 (2020).

Appendix A: Non-uniqueness of the representation of \mathcal{L}_t

Any time-local generator that is trace- and hermiticity-preserving can be written in the following form (compare with Eq.(1))

$$\mathcal{L}_t(\rho) = -i[H(t), \rho] + \mathcal{J}_t(\rho) - \frac{1}{2}\{\Gamma(t), \rho\}, \quad (\text{A1})$$

with

$$\Gamma(t) = \mathcal{J}_t^\dagger(\mathbb{1}) \quad (\text{A2})$$

($\mathbb{1}$ is the identity operator) and \mathcal{J}_t a linear hermiticity-preserving map, that is, $\mathcal{J}_t(X^\dagger) = (\mathcal{J}_t(X))^\dagger$. Obviously, this representation is not unique. One may define a new map

$$\mathcal{J}'_t(\rho) = \mathcal{J}_t(\rho) + \frac{1}{2}(A(t)\rho + \rho A^\dagger(t)), \quad (\text{A3})$$

with arbitrary $A(t) = A_1(t) + iA_2(t)$ (and Hermitian $A_k(t)$ $k = 1, 2$), together with

$$H'(t) = H(t) + \frac{1}{2}A_2(t) \quad (\text{A4})$$

and

$$\Gamma'(t) = \Gamma(t) + A_1(t), \quad (\text{A5})$$

giving rise to the same generator

$$\mathcal{L}_t(\rho) = -i[H'(t), \rho] + \mathcal{J}'_t(\rho) - \frac{1}{2}\{\Gamma'(t), \rho\}, \quad (\text{A6})$$

and still such that $\Gamma'(t) = \mathcal{J}'_t(\mathbb{1})$ and \mathcal{J}'_t is a linear hermiticity-preserving map.

Note, that the rate operator \mathbf{W}_ψ does not depend on the particular representation. Indeed, one has

$$\mathbf{W}_\psi = (\mathbb{1} - P_\psi)\mathcal{L}(P_\psi)(\mathbb{1} - P_\psi) = (\mathbb{1} - P_\psi)\mathcal{J}(P_\psi)(\mathbb{1} - P_\psi) = (\mathbb{1} - P_\psi)\mathcal{J}'(P_\psi)(\mathbb{1} - P_\psi). \quad (\text{A7})$$

However, the rate operator \mathbf{R}_ψ is defined for a given representation

$$\mathbf{R}_\psi = \mathcal{J}_t(P_\psi). \quad (\text{A8})$$

If the generator is dissipative, then there exists representation for which the map \mathcal{J}_t is positive and hence $\mathbf{R}_\psi \geq 0$ for all $|\psi\rangle$.

Appendix B: Proof that R-ROQJ is a proper unraveling of the master equation (1)

Let us recall that the R-ROQJ unraveling is defined as the deterministic evolution fixed by Eq.(2), with

$$K(t) = H(t) - \frac{i}{2}\Gamma(t), \quad (\text{B1})$$

interrupted by the jumps in Eq.(11), each of them occurring in the time interval between t and $t + dt$ with probability (12), conditioned on having the state $|\psi(t)\rangle$ at time t before the (possible) jump. Moreover, the jump operator is defined as

$$R_{\psi(t),k} = \sqrt{r_{\psi(t),k}}|\phi_{\psi(t),k}\rangle\langle\psi(t)|, \quad (\text{B2})$$

where $r_{\psi(t),j}$ and $|\phi_{\psi(t),k}\rangle$ are the eigenvalues and normalized eigenvectors of $\mathbf{R}_{\psi(t)}$ defined by Eq.(10), i.e.,

$$\mathbf{R}_{\psi(t)} = \mathcal{J}_t(|\psi(t)\rangle\langle\psi(t)|) = \sum_{k=1}^N r_{\psi(t),k}|\phi_{\psi(t),k}\rangle\langle\phi_{\psi(t),k}|; \quad (\text{B3})$$

indeed the R-ROQJ is defined for a positive rate operator $\mathbf{R}_{\psi(t)}$, i.e., for $r_{\psi(t),k} \geq 0$ for any $\psi(t)$ and k .

Now, given the pure state $|\psi(t)\rangle\langle\psi(t)|$ at time t , the deterministic evolution will occur with probability

$$P_{\psi(t)}^{det} = 1 - \sum_{k=1}^N p''_{\psi(t),k} = 1 - \sum_{k=1}^N r_{\psi(t),k} dt = 1 - \text{Tr} \{ \mathbf{R}_{\psi(t)} \} dt, \quad (\text{B4})$$

where in the last equality Tr denotes the trace and we used Eq.(B3). But using once again Eq.(B3) (the first equality), along with Eq.(A2), we get

$$P_{\psi(t)}^{det} = 1 - \text{Tr} \{ \mathcal{J}_t(|\psi(t)\rangle\langle\psi(t)|) \} dt = 1 - \text{Tr} \left\{ |\psi(t)\rangle\langle\psi(t)| \mathcal{J}'_t(\mathbb{1}) \right\} dt = 1 - \langle\psi(t)|\Gamma(t)|\psi(t)\rangle dt. \quad (\text{B5})$$

In addition, the deterministic evolution will map the pure state $|\psi(t)\rangle\langle\psi(t)|$ into the pure state (see Eq.(2))

$$\frac{(1 - iK(t)dt)|\psi(t)\rangle\langle\psi(t)|(1 + iK^\dagger(t)dt)}{\|(1 - iK(t)dt)|\psi(t)\rangle\|^2} = \frac{(1 - iK(t)dt)|\psi(t)\rangle\langle\psi(t)|(1 + iK^\dagger(t)dt)}{1 - \langle\psi(t)|\Gamma(t)|\psi(t)\rangle dt} = \frac{(1 - iK(t)dt)|\psi(t)\rangle\langle\psi(t)|(1 + iK^\dagger(t)dt)}{P_{\psi(t)}^{det}}, \quad (\text{B6})$$

where in the first equality we used Eq.(B1) in the denominator (and neglected the terms of order dt^2), while in the second equality we used Eq.(B5).

On the other hand, as said, given the state $|\psi(t)\rangle\langle\psi(t)|$ at time t , we will have the jump described by $R_{\psi(t),k}$ in Eq.(B2), i.e. (compare with Eq.(11))

$$|\psi(t)\rangle\langle\psi(t)| \rightarrow \frac{R_{\psi,k}|\psi(t)\rangle\langle\psi(t)R_{\psi,k}^\dagger}{\|R_{\psi,k}|\psi(t)\rangle\|^2} = |\phi_{\psi(t),k}\rangle\langle\phi_{\psi(t),k}|, \quad (\text{B7})$$

with probability as in Eq.(12).

All in all, if we average the state at time $t + dt$ over the trajectories where the state at time t is $|\psi(t)\rangle\langle\psi(t)|$, we get the mixture of the states obtained via the deterministic evolution or one of the jumps, each weighted with the corresponding probability: using Eqs.(B6), (B7) and (12), such a (conditioned) average corresponds to

$$\begin{aligned} & \frac{P_{\psi(t)}^{det} (1 - iK(t)dt)|\psi(t)\rangle\langle\psi(t)|(1 + iK^\dagger(t)dt)}{P_{\psi(t)}^{det}} + \sum_{k=1}^N r_{\psi(t),k} |\phi_{\psi(t),k}\rangle\langle\phi_{\psi(t),k}| dt \\ &= |\psi(t)\rangle\langle\psi(t)| - i [H, |\psi(t)\rangle\langle\psi(t)|] dt - \frac{1}{2} \{\Gamma(t), |\psi(t)\rangle\langle\psi(t)|\} dt + \mathcal{J}_t(|\psi(t)\rangle\langle\psi(t)|) dt, \end{aligned} \quad (\text{B8})$$

where the equality is due to Eqs.(B1) and (B3), and we neglected the terms of order dt^2 . Finally, we perform a second average, this time with respect to the pure states $|\psi(t)\rangle\langle\psi(t)|$ we fixed at time t , so that we get the average over all the trajectories; the previous expression then yields the first order expansion of the time-local master equation $d\rho(t)/(dt) = \mathcal{L}_t(\rho(t))$ with \mathcal{L}_t as in Eq.(1), which concludes the proof.

Indeed, the proof above does not depend on the specific representation of the generator \mathcal{L}_t (see the previous section) and then it holds for any \mathcal{J}_t , along with the $\Gamma(t)$ defined in Eq.(A2), as long as the corresponding rate operator $\mathbf{R}_{\psi(t)}$ is positive.

Appendix C: Proof of Proposition 1

The proof easily follows from the well known min-max principle for Hermitian matrices: let A be a Hermitian $n \times n$ matrix, and let

$$\lambda_n \geq \lambda_{n-1} \geq \dots \geq \lambda_1$$

be the real eigenvalues of A . Then

$$\lambda_k = \max_{\Sigma} \min_{x \in \Sigma} \langle x | A | x \rangle \quad (\text{C1})$$

where x is normalized, and Σ is a $(n - k + 1)$ -dimensional subspace of \mathbb{C}^n .

Now, since $\mathbf{W}_\psi = (\mathbb{1} - P)\mathbf{R}_\psi(\mathbb{1} - P) \geq 0$, one has for any $x \in \Sigma = (\mathbb{1} - P)\mathbb{C}^n$

$$\langle x | \mathbf{R}_\psi | x \rangle = \langle x | \mathbf{W}_\psi | x \rangle \geq 0.$$

Hence, from (C1) one finds $\lambda_2 \geq 0$ (since in (C1) one maximizes over all Σ s), and hence only λ_1 may be negative.

Appendix D: Proof that \mathbf{J}_t in Eq.(15) defines a positive map

Defining

$$\mathbf{K}(t) = \int_{U(N)} \mathcal{L}_t^\dagger(U^\dagger) U dU, \quad (\text{D1})$$

one finds for an arbitrary $V \in U(N)$

$$\int_{U(N)} \mathcal{L}_t^\dagger(VU^\dagger) U dU = \int_{U(N)} \mathcal{L}_t^\dagger(U'^\dagger) U' V dU' = \mathbf{K}(t)V, \quad (\text{D2})$$

with $U' = UV^\dagger$. Hence for an arbitrary system operator X one has

$$\int_{U(N)} \mathcal{L}_t^\dagger(XU^\dagger) U dU = \mathbf{K}(t)X. \quad (\text{D3})$$

Now we use the dissipativity condition

$$\mathcal{L}_t^\dagger(Y^\dagger Y) \geq \mathcal{L}_t^\dagger(Y^\dagger) Y + Y^\dagger \mathcal{L}_t^\dagger(Y), \quad (\text{D4})$$

for $Y = UX$, with $U \in U(N)$. It leads to

$$\mathcal{L}_t^\dagger(Y^\dagger Y) \geq \mathcal{L}_t^\dagger(X^\dagger U^\dagger)UX + X^\dagger U^\dagger \mathcal{L}_t^\dagger(UX) = \mathcal{L}_t^\dagger(X^\dagger U^\dagger)UX + X^\dagger [\mathcal{L}_t^\dagger(X^\dagger U^\dagger)U]^\dagger. \quad (\text{D5})$$

Averaging over $U(N)$ yields

$$\int_{U(N)} \mathcal{L}_t^\dagger(Y^\dagger Y) dU \geq \int_{U(N)} \mathcal{L}_t^\dagger(X^\dagger U^\dagger)U dU X + X^\dagger \left(\int_{U(N)} \mathcal{L}_t^\dagger(X^\dagger U^\dagger)U dU \right)^\dagger = \mathbf{K}(t)X^\dagger X + X^\dagger X \mathbf{K}^\dagger(t), \quad (\text{D6})$$

and hence defining a linear map as in Eq.(15),

$$\mathbf{J}_t^\dagger(X) = \mathcal{L}_t^\dagger(X) - (\mathbf{K}(t)X + X\mathbf{K}^\dagger(t)), \quad (\text{D7})$$

we have shown that

$$\mathbf{J}_t^\dagger(X^\dagger X) \geq 0, \quad (\text{D8})$$

which proves that the map \mathbf{J}_t is positive.

Appendix E: Positivity of the rate operators $\mathbf{R1}_{\psi(t)}$ and $\mathbf{R2}_{\psi(t)}$

The qubit generator

$$\mathcal{L}_t(\rho) = \frac{1}{2} \sum_{k=1}^3 \gamma_k(t) (\sigma_k \rho \sigma_k - \rho), \quad (\text{E1})$$

may be rewritten as

$$\mathcal{L}_t(\rho) = \sum_{k=1}^3 \gamma_k(t) (J_k(\rho) - \rho), \quad (\text{E2})$$

where

$$J_k(\rho) = \frac{1}{2} (\sigma_k \rho \sigma_k + \rho), \quad (\text{E3})$$

are CPTP for $k = 1, 2, 3$. The following map, i.e., Eq. (17),

$$\mathbf{J}_t(\rho) = \sum_{k=1}^3 \gamma_k(t) (J_k(\rho) + \rho) = \mathcal{J}_t(\rho) + \gamma(t)\rho, \quad (\text{E4})$$

is positive for $\gamma_1 = \gamma_2 = 1$ and $\gamma_3(t) = -\tanh t$. The proof is based on the following observation: for a qubit system a linear map $\Phi : M_2(\mathbb{C}) \rightarrow M_2(\mathbb{C})$ is positive if and only the corresponding Choi matrix C_Φ

$$C_\Phi := \sum_{i,j=1}^2 |i\rangle\langle j| \otimes \Phi(|i\rangle\langle j|)$$

satisfies

$$C_\Phi = A + (\mathbb{1} \otimes T)B,$$

where A and B are positive 4×4 matrices, and ‘ $\mathbb{1} \otimes T$ ’ denotes partial transposition. The Choi matrix for the map \mathbf{J}_t reads

$$C_{\mathbf{J}_t} = \left(\begin{array}{cc|cc} 2(1 - \tanh t) & 0 & 0 & 2 \\ 0 & 2 & 0 & 0 \\ \hline 0 & 0 & 2 & 0 \\ 2 & 0 & 0 & 2(1 - \tanh t) \end{array} \right) = A + (\mathbb{1} \otimes T)B, \quad (\text{E5})$$

with

$$A = \left(\begin{array}{cc|cc} 2(1 - \tanh t) & 0 & 0 & 0 \\ 0 & 0 & 0 & 0 \\ \hline 0 & 0 & 0 & 0 \\ 0 & 0 & 0 & 2(1 - \tanh t) \end{array} \right), \quad B = \left(\begin{array}{cc|cc} 0 & 0 & 0 & 0 \\ 0 & 2 & 2 & 0 \\ \hline 0 & 2 & 2 & 0 \\ 0 & 0 & 0 & 0 \end{array} \right). \quad (\text{E6})$$

It is evident that both A and B are positive, which proves positivity of the map \mathbf{J}_t and hence $\mathbf{R}\mathbf{1}_{\psi(t)} \geq 0$.

Similarly one may prove that $\mathbf{R}\mathbf{2}_{\psi(t)} \geq 0$. In this case the corresponding Choi matrix reads

$$C_{\mathbf{J}_t} = \left(\begin{array}{cc|cc} 2 & 0 & 0 & 2(1 + \tanh t) \\ 0 & 2 & 0 & 0 \\ \hline 0 & 0 & 2 & 0 \\ 2(1 + \tanh t) & 0 & 0 & 2 \end{array} \right) = A' + (\mathbf{1} \otimes T)B', \quad (\text{E7})$$

with

$$A' = \left(\begin{array}{cc|cc} 2 & 0 & 0 & 2 \\ 0 & 0 & 0 & 0 \\ \hline 0 & 0 & 0 & 0 \\ 2 & 0 & 0 & 2 \end{array} \right), \quad B' = \left(\begin{array}{cc|cc} 0 & 0 & 0 & 0 \\ 0 & 2 & 2 \tanh t & 0 \\ \hline 0 & 2 \tanh t & 2 & 0 \\ 0 & 0 & 0 & 0 \end{array} \right). \quad (\text{E8})$$

Appendix F: Positivity of \mathbf{J}_t for the phase covariant master equation

Consider the phase-covariant generator (compare with Eq.(20))

$$\mathcal{L}_t(\rho) = -i\frac{\omega(t)}{2}[\sigma_z, \rho] + \gamma_+(t)\mathcal{L}_+(\rho) + \gamma_-(t)\mathcal{L}_-(\rho) + \gamma_z(t)\mathcal{L}_z(\rho), \quad (\text{F1})$$

where $\mathcal{L}_{\pm}(\rho) = \sigma_{\pm}\rho\sigma_{\mp} - \frac{1}{2}\{\sigma_{\mp}\sigma_{\pm}\rho\}$ and $\mathcal{L}_z(\rho) = \sigma_z\rho\sigma_z - \rho$. This generator gives rise to a P-divisible evolution if and only if

$$\gamma_+(t) \geq 0, \quad \gamma_-(t) \geq 0, \quad \sqrt{\gamma_+(t)\gamma_-(t)} + 2\gamma_z(t) \geq 0. \quad (\text{F2})$$

Now, suppose that $\gamma_z(t) < 0$. We prove that the map

$$\mathbf{J}_t(\rho) = (\gamma_+(t)\sigma_+\rho\sigma_- + \gamma_-(t)\sigma_-\rho\sigma_+ + \gamma_z(t)\sigma_z\rho\sigma_z) + \frac{1}{2}[\gamma_+(t) + \gamma_-(t) + 2\gamma_z(t)]\rho \quad (\text{F3})$$

is positive, as long as Eq.(F2) is satisfied. The corresponding Choi matrix reads (we skip the time dependence)

$$C = \left(\begin{array}{cc|cc} \gamma_z & 0 & 0 & -\gamma_z \\ 0 & \gamma_+ & 0 & 0 \\ \hline 0 & 0 & \gamma_- & 0 \\ -\gamma_z & 0 & 0 & \gamma_z \end{array} \right) + \left(\frac{\gamma_+ + \gamma_-}{2} + \gamma_z \right) \left(\begin{array}{cc|cc} 1 & 0 & 0 & 1 \\ 0 & 0 & 0 & 0 \\ \hline 0 & 0 & 0 & 0 \\ 1 & 0 & 0 & 1 \end{array} \right), \quad (\text{F4})$$

and hence

$$C = X + (\mathbf{1} \otimes T)Y,$$

with

$$X = \left(\begin{array}{cc|cc} a+b & 0 & 0 & a \\ 0 & 0 & 0 & 0 \\ \hline 0 & 0 & 0 & 0 \\ a & 0 & 0 & a+b \end{array} \right), \quad Y = \left(\begin{array}{cc|cc} 0 & 0 & 0 & 0 \\ 0 & \gamma_+ & \sqrt{\gamma_+\gamma_-} & 0 \\ \hline 0 & \sqrt{\gamma_+\gamma_-} & \gamma_- & 0 \\ 0 & 0 & 0 & 0 \end{array} \right), \quad (\text{F5})$$

and

$$a = \frac{\gamma_+ + \gamma_-}{2} - \sqrt{\gamma_+\gamma_-}, \quad b = \sqrt{\gamma_+\gamma_-} + 2\gamma_z;$$

X and Y are easily shown to be positive under the validity of Eq.(F2).

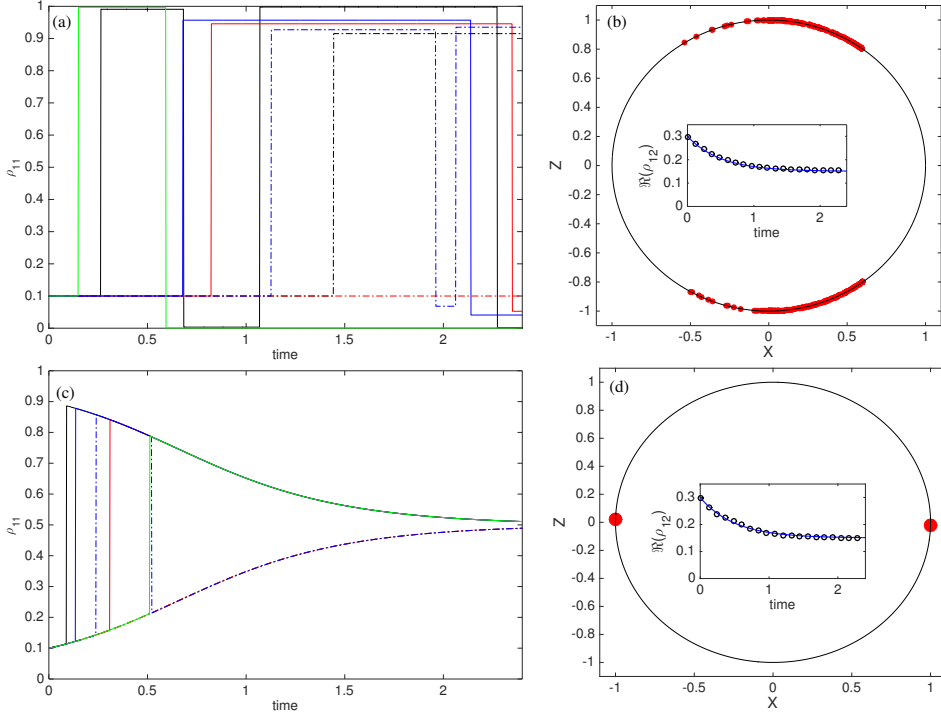


Figure 2. (Color online) Simulation results using rate operator **R3** [(a), (b)] and **W** [(c), (d)]. Seven example pure state trajectories are displayed in (a) and (c) by plotting the probability of state $|1\rangle$. Final steady state distributions for Bloch vector X and Z components, with 500 trajectories, are shown in (b) and (d). Here, each dot corresponds to single trajectory. In (d), all the 500 dots have the value $Z = 0$ and $X = -1/2$ or $X = +1/2$, i.e., we have only two distinctively visible dots. The insets in (b) and (d) demonstrate the agreement between the analytical and simulation results by using the coherence ρ_{12} and having 10^4 trajectories. In the insets, the solid line is the analytical result and the dots are the simulation results. The error bars are similar to the size of the dots. In all the panels, the initial state is $|\psi(0)\rangle = \sqrt{0.1}|1\rangle + \sqrt{0.9}|2\rangle$ and the used time step size is $dt = 0.002$.

Appendix G: Unraveling of the ENM master equation with **R3** and **W**

In the main text we showed the simulation results for the ENM master equation (16) with rates $\gamma_1 = \gamma_2 = 1$, and $\gamma_3(t) = -\tanh t$ and using the rate operators **R1** [cf. (18)] and **R2** [cf. (19)]. In the following, we will define yet another positive rate operator **R3** and display the corresponding simulation results for this and also for **W** [cf. (5)]. Moreover, we describe further the differences between all of the used operators.

So, consider the rate operator

$$\mathbf{R3}_\psi = \frac{1}{2} \sum_{k=1}^3 \gamma_k(t) \sigma_k |\psi(t)\rangle \langle \psi(t)| \sigma_k - \frac{1}{2} \gamma_3(t) |\psi(t)\rangle \langle \psi(t)|, \quad (\text{G1})$$

that is positive as we subtract a negative operator proportional to the projector $P_{\psi(t)}$, $\gamma_3(t) < 0$. The corresponding deterministic evolution is fixed by the linear operator $K3(t) = \frac{i}{4} [\gamma_1(t) + \gamma_2(t)] \mathbb{1}$. We show the simulation results in Fig. 2 (a) and (b) with the same used initial state as in the main text. The example realizations in Fig. 2 (a) demonstrate that, similarly to **R1** (cf. Fig. 1), the jumps continue even though the steady state has been reached. However, contrary to **R1**, now it holds all the time that $\rho_{11} \leq 0.1$ or $\rho_{11} \geq 0.9$. This can be seen more clearly in Fig. 2 (b). While the distribution of trajectories in steady state for **R1** contained arcs on western and eastern side of the XZ -plane of the Bloch sphere, now with **R3** the distribution covers arcs on northern and southern sides of the circle. As before, there is excellent agreement between the analytical and simulation results [see the inset of Fig. 2 (b).]

The last operator we consider is **W**, see Eq. (5). We display the simulation results in Fig. 2 (c) and (d). With the example realizations in Fig. 2 (c), one can clearly see that now also the deterministic evolution changes the states. Moreover, the jumps happen between a pair of states only and terminate when the steady state is reached. Fig. 2 (d)

Rate operator	Asymptotic jumps?	Deterministic changes?	Time-independent measurement basis?	Effective ensemble size
R1	yes	no	no	∞
R2	no	no	yes	3
R3	yes	no	no	∞
W	no	yes	no	2

Table I. The basic characterization of the four used rate operators for stochastic simulations. Quantum jumps can either continue or terminate when steady state is reached. Depending on the form of the effective Hamiltonian giving the deterministic evolution, the state of the trajectory can either change or remain unchanged after renormalization. The measurement basis for the measurement scheme interpretation can be either time-dependent or time-independent. The effective ensemble size describes how many different kinds of state vectors the ensemble consists of point-wise in time.

shows that similarly to **R2** [cf. Fig. 1 (d)], all the trajectories eventually end up being on one of the two states on the equator of the Bloch sphere. However, how they reach these points is totally different that with **R2**. In terms of the measurement scheme, there is another crucial difference between **W** and **R2**. With **W** the measurement basis is time-dependent, while with **R2** it is time independent.

Table I collects and compares the properties of all the used four operators in terms of (i) whether the quantum jumps continue also in the asymptotic regime or terminate when the steady state is reached, (ii) whether the deterministic evolution changes the state of the trajectories, (iii) whether the measurement basis is time-dependent or time-independent, and (iv) what is the effective ensemble size in the simulation (how many different kinds of state vectors the ensemble consists of point-wise in time). Overall, the rate operator **R2** has the most appealing properties from simulation and fundamental interpretation points of views.